Materials and Design 43 (2013) 492–498

Contents lists available at SciVerse ScienceDirect

Materials and Design

journal homepage: www.elsevier.com/locate/matdes

A novel severe plastic deformation method for fabricating ultrafine grained pure copper

Chengpeng Wang *, Fuguo Li, Qinghua Li, Jiang Li, Lei Wang, Junzhe Dong

State Key Laboratory of Solidification Processing, School of Materials Science and Engineering, Northwestern Polytechnical University, Xi'an 710072, PR China

ARTICLE INFO

Article history:
Received 19 April 2012
Accepted 20 July 2012
Available online 28 July 2012

Keywords:
A. Non-ferrous metals and alloys
C. Extrusion
F. Microstructure
G. Optical microscopy

ABSTRACT

A novel severe plastic deformation (SPD) method entitled elliptical cross-section spiral equal-channel extrusion (ECSEE) was proposed to fabricate ultrafine grained (UFG) pure copper. The principle of ECSEE process was adopted to accumulate shear stress within the workpiece without any cross-section area change. In order to primarily demonstrate the deformation characteristic and refinement ability of ECSEE method, the simulated and experimental investigations were both done. In the case of simulation, the ECSEE-ed workpiece containing scribed grids was analyzed for the flow net change. Simulated results indicated the trend of effective strain distribution decreased from the circumferential area to the central area on the cross-section of ECSEE-ed workpiece. In experimental investigations of a single-pass of ECSEE, a significant grain refinement from 10–50 μm to 1–10 μm was mainly in the circumferential area of the cross-section for processed workpieces. During the ECSEE deformation, shear strain as an essential role conduced the grain refinement. Besides, a significant increase of hardness, from ~40 Hv to ~85 Hv, was examined. The distribution characteristic of refinement and hardness were both consistent with that of simulated effective strain.

1. Introduction

Ultrafine grained (UFG) or nanostructural materials are well known due to their high strength and unique properties. Among different approaches of fabricating these materials, severe plastic deformation (SPD) methods are of more interest as they provide UFG or even bulk nanostructural materials without contamination or porosity [1,2]. In the last decades, the most common SPD methods included equal channel angular pressing (ECAP) [3], high pressure torsion (HPT) [4], cyclic extrusion compression (CEC) [5], twist extrusion (TE) [6,7], accumulated roll bonding (ARB) [8] and constrained groove pressing (CGP) [9], etc. Nowadays, SPD technology is emerging from the domain of laboratory-scale research into the commercial fabrication of various UFG materials [1,2]. Therefore, further studies are necessary to conducted on commercializing these SPD methods [10,11]. To simplify and improve these processing operations or to achieve unique properties of materials processed by SPD, some efforts have been made on the modifications of these methods [12–18].

In all the SPD methods, TE technique is becoming a hotspot of the most promising industrial SPD method [6,7]. However, the non-symmetric nature of processing restricts its application to only the rectangular section of blank [19]. Industrial raw materials are basically circular section shape. Thus, the tedious process design of TE is probably restricted in the industrial application.

In order to overcome the aforementioned lacks of TE technique, a novel SPD method named elliptical cross-section spiral equal-channel extrusion (ECSEE) was proposed in this paper. ECSEE method can be facilely utilized on any standard extrusion equipments to accumulate torsion deformation for the material refinement. Moreover, reversing the harmful friction into the impetus of SPD is one of the advantages for ECSEE.

To study the flow behavior of the material in ECSEE, a simulated deformation grid of the transverse plane was observed using the flow net analysis of the finite element software, DEFORM-3D. Subsequently, both effective strains of plane distribution and tracking points were examined through FEM. In order to primarily demonstrate its refinement and applicability, the commercial pure copper was executed by one pass of ECSEE processing, and the experimental investigations of metallographic and hardness were executed.

2. Principle of ECSEE

A schematic diagram of the ECSEE technique is shown in Fig. 1. A round-bar workpiece is extruded out through a die with three channel regions: round–ellipse cross-section transitional channel L_1, elliptical cross-section torsion transitional channel L_2 and ellipse–round cross-section transitional channel L_3. Due to the

* Corresponding author. Tel.: +86 29 88474117; fax: +86 29 88492642.
E-mail addresses: cpwang@mail.nwpu.edu.cn (C. Wang), fuguolx@nwpu.edu.cn (F. Li).

0261-3069/$ - see front matter © 2012 Elsevier Ltd. All rights reserved.
http://dx.doi.org/10.1016/j.matdes.2012.07.047

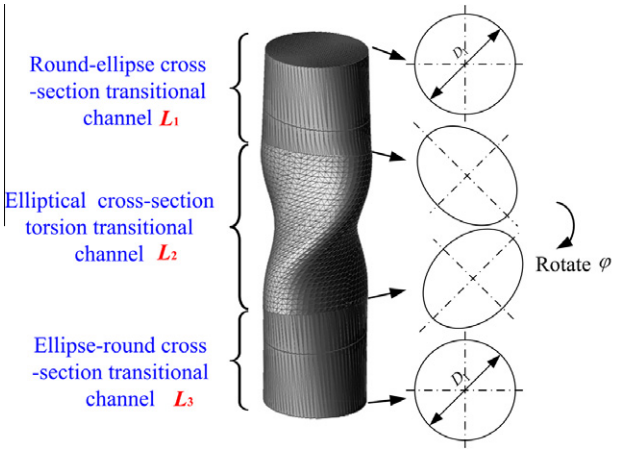

Fig. 1. Schematic diagram of ECSEE.

special shape of die channel, the ECSEE-ed workpiece is subjected to a severe plastic deformation, while the cross-section area remains constant. This feature allows the workpiece to be extruded repeatedly for the deformation accumulation, which is essential to refine the microstructure and improve the property of materials [2].

According to the principle of ECSEE, the deformation can be identified as two basic forms: the round–ellipse/ellipse–round cross-section transitional channel deformation and the elliptical cross-section torsion transitional channel deformation. These are mainly generated from the channel L_1/L_3 and L_2, respectively. Considering the channel L_2 displays a more significant influence on the accumulation of severe shear deformation than the counterpart of the channel L_1 and L_3, so only to study the former.

Simply, the torsion deformation of the channel L_2 is considered as the counterpart of a cylinder with an elliptic-section and unchanged height L_2 which is twisted in such a way that the top surface is rotated through an angle φ with respect to the lower surface (Fig. 2). Assume the minor-axis length is R, and m is the ratio of major-axis and minor-axis length of the elliptic-section, so the major-axis length is expressed as mR. According to the unchanged cross-section area of die channel, the following relationship is obtained.

$$\frac{\pi D_1^2}{4} = \frac{\pi m R^2}{4} \tag{1}$$

$$R = \frac{\sqrt{m} D_1}{m} \tag{2}$$

where D_1 is the diameter of round cross-section of the workpiece before and after ECSEE deformation.

Assume the deformed body is in a state of simple shear. Since the state of strain is not homogeneous, and varies with the radial position of the element considered, the corresponding strain distribution is similarly non-uniform. To calculate the strain in the channel L_2 during the ECSEE processing, the initially a planar section normal to the extrusion direction is studied. Generally, the total torsion shear strain consists of both plastic one and elastic one. However, for high plastic materials, the elastic shear strain is ignored, and the plastic shear one is approximately equal to the total one. Therefore, the maximal shear strain γ_{max} on the circumferential surface of one single-pass processed workpiece is given by:

$$\gamma_{max} = \tan\alpha = \frac{\varphi m R}{2L_2} = \frac{\varphi\sqrt{m} D_1}{2L_2} \tag{3}$$

where α is a torsion angle for the straight line parallel to the axis on the surface under the shear strain γ_{max}.

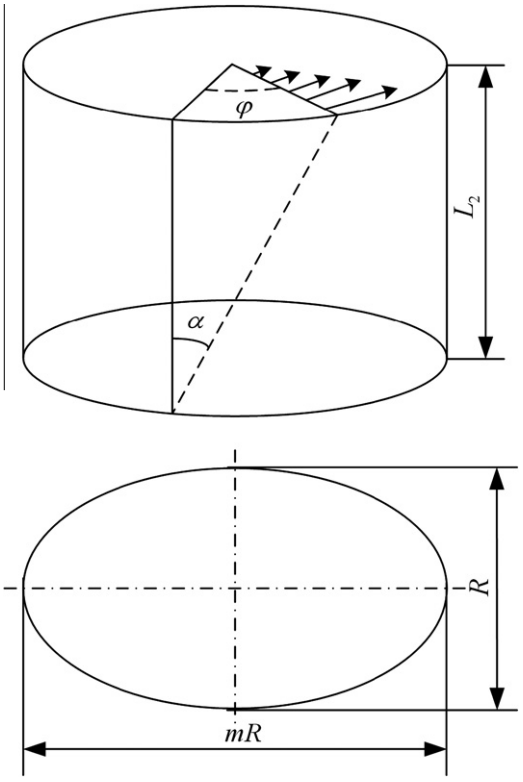

Fig. 2. Illustration of a planar section of specimen normal to torsion extrusion direction.

According to Mises criterion, the corresponding maximal strain value can be calculated as well:

$$\varepsilon_{max} = \frac{\gamma_{max}}{\sqrt{3}} = \frac{\varphi\sqrt{3m} D_1}{6L_2} \tag{4}$$

The theoretical value of strain in one single-pass of ECSEE is expected to be high for the grain refinement. Based on Eqs. (3) and (4), it is possible to attain different effective strain values per pass by changing three primary parameters: the rotation angle φ, the channel L_2 and the diameter D_1. In practice, it is impossible to obtain an extreme high strain due to the required critical damage/crack and actual processing conditions.

3. Simulated and experimental procedure

By means of DEFORM-3D V6.1 software, finite element simulation was carried out for cold extrusion with the plastic deformation behavior of the materials [20], as:

$$\bar{\sigma} = k\bar{\varepsilon}^n \tag{5}$$

where $\bar{\sigma}$ is the effective Von-misses stress, $\bar{\varepsilon}$ is the effective plastic strain, k is the strength coefficient and n is the strain hardening exponent.

According to the National Standard of China GB/T 228-2002 [21], the workpieces of the commercial pure copper (99.7 wt.%) were determined experimentally by PWS-1000 universal compression test at room temperature and the strain rate of 0.01/s. Then the experimental data were analyzed and obtained the parameters of k = 432 MPa and n = 0.31 in Eq. (5). The workpieces used for the finite element model were 10 mm in diameter and 35 mm in length, the rigid upper was a rod punch with the diameter 10 mm, the extrusion die channel was a set as: D_1 = 10 mm, L_1 = 7 mm, L_2 = 10 mm, L_3 = 7 mm, φ = 90° and m = 1.55. Note that

the cross-section area of the die channel is constant, whether for the round one or the elliptical one.

With the aim of full recrystallization uniform annealing, the experimental workpieces of pure copper were pretreated by annealing at 650 °C for 2 h and furnace cooling [22]. Refer to the related literature about the extrusion speed of ECAP [23], the extrusion test was performed on the YA32-315 hydraulic press with the speed of 1 mm/s and the lard lubrication.

Subsequently, the pretreated workpieces were wire-cut (the cutting positions shown in Fig. 3), grinded at the waterproof abrasive papers, and mechanical polished with diamond powder. The prepared workpieces were etched in 1 g $FeCl_3$, 3 ml HCl and 20 ml H_2O for 10 s to reveal the microstructure morphology. Microstructure of polished workpieces surface was examined by using an Olympus PMG3 optical microscope.

The Vickers microhardness tests were employed under HXP-1000TM microhardness tester in a load of 100 g and a dwell time of 15 s, following the Chinese national standards GB/T 4340.1-2009 [24]. As shown in Fig. 3, the measured points of hardness were symmetrically selected starting from the center point to the center point along the contour of the workpiece cross-section in an anticlockwise direction. All the hardness values were measured five times, and then taken the average.

4. Results and discussions

4.1. Effective strain distribution

The effective strain distribution on a random cross-section of the workpiece deformed in channel L_2 is shown in Fig. 4. The effective strain value of the circumferential part is high, even more than 1.1, while the counterpart of the central part is low, only in the range of 0.18–0.37. The value gradually decreases from the circumferential area to the central area. A very obvious strain gradient distribution is found on the workpiece cross-section. This decreasing trend of effective strain distribution is similar to the counterpart of TE research. Beygelzimer et al. [6] found that a strain gradient distribution existed in the TE deformation behavior based on the rotational and translational flow fields.

ECSEE mainly generated from the torsion die channel L_2 utilizes the combination of shear strain and pressure stress to accumulate strain for severe plastic deformation. Generally, the strain distribution on the cross-section of a torsion bar is inhomogeneous. It is reasonable to anticipate from Eq. (4) that the effective strain distribution introduced by ECSEE will be extremely inhomogeneous. The possibility of achieving a gradual evolution towards a homogeneous strain on the cross-section of ECSEE-ed workpieces is

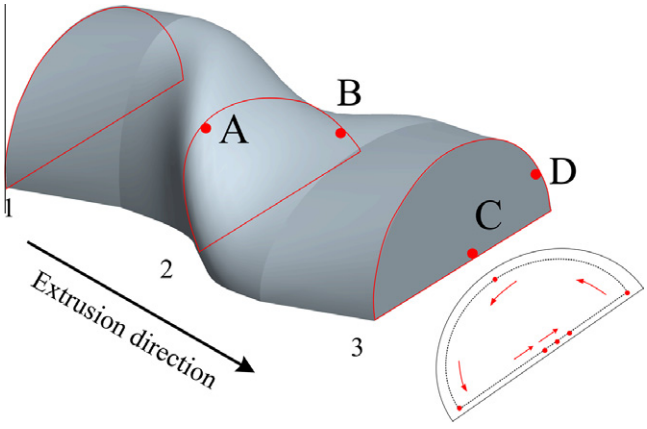

Fig. 3. Cutting positions and selected locations of the metallographic observations and microhardness tests.

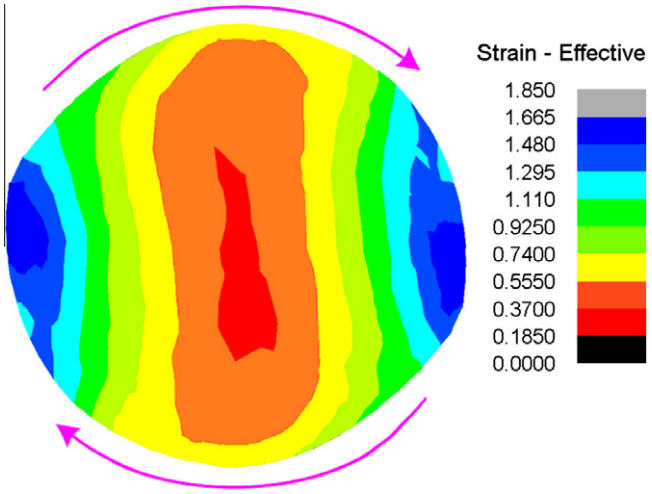

Fig. 4. The simulated effective strain distribution of the cross-section.

processed by increasing either the applied rotation angle φ and/or the ratio of major-axis length and minor-axis length m, which is equivalent to increasing torque for the torsion of ECSEE. One can imagine that increasing the total numbers of revolution is good for the homogeneous strain of ECSEE.

In addition, the ellipse shape of distribution is matched with the elliptical cross-section shape of the ECSEE die channel L_2. The value of effective strain in left–right area is higher than that of the up–down area. This especial distribution pattern is possibly due to the severe shear deformation in the major-axis area of the elliptical cross-section, while the minor-axis area is subjected to a less shear deformation. The asymmetry cross-section shape of the channel L_2 is probable the reason of inhomogeneous effective strain distribution. According to Eq. (4), the ratio of major-axis length and minor-axis length m is essential to the strain distribution pattern. High value of m for the bigger elliptic rate can increase the torque, so the strain distribution is more inhomogeneous. In addition, the effective strain rotates with the plane torsion in the clockwise direction. The more obvious "vortex" phenomenon is the closer the strain is to the circumferential area.

4.2. Effective strain of tracking points

Fig. 5 shows, at the final forming stage, the effective strain distribution of tracking points along the diameter direction through the center point of cross-section and the circumference direction, respectively. As shown in Fig. 5b, the distribution curve of effective strain of tracking points along the circumferential direction presents an oval shape, which is consistent with the cross-section shape of the ECSEE die channel L_2. Note that the tracking points only are chosen from a half cross-section of the channel, and the other half is artificially symmetry. The two variations of effective strain are both corresponding to the top curve above the dotted line and the bottom one under the dotted line, respectively.

For the effective strain of radial distribution (Fig. 5c), the value of central part is low, while the circumferential one is high. The results are consistent with the observations of effective strain distribution in the above-mentioned Section 4.1. That is also indicated that the ECSEE deformation in the cross-section of workpieces is an inhomogeneous deformation. Similar research was also reported in the deformation pattern of TE and HPT. For example, a 3D strain distribution established by Zhilyaev et al. [25] displays a smooth increase in the total strain from the center to the periphery on the cross-section of HPT-ed samples. The reason of special effective strain distribution pattern may be explained by the torsion deformation of the unique ellipse cross-section of ECSEE

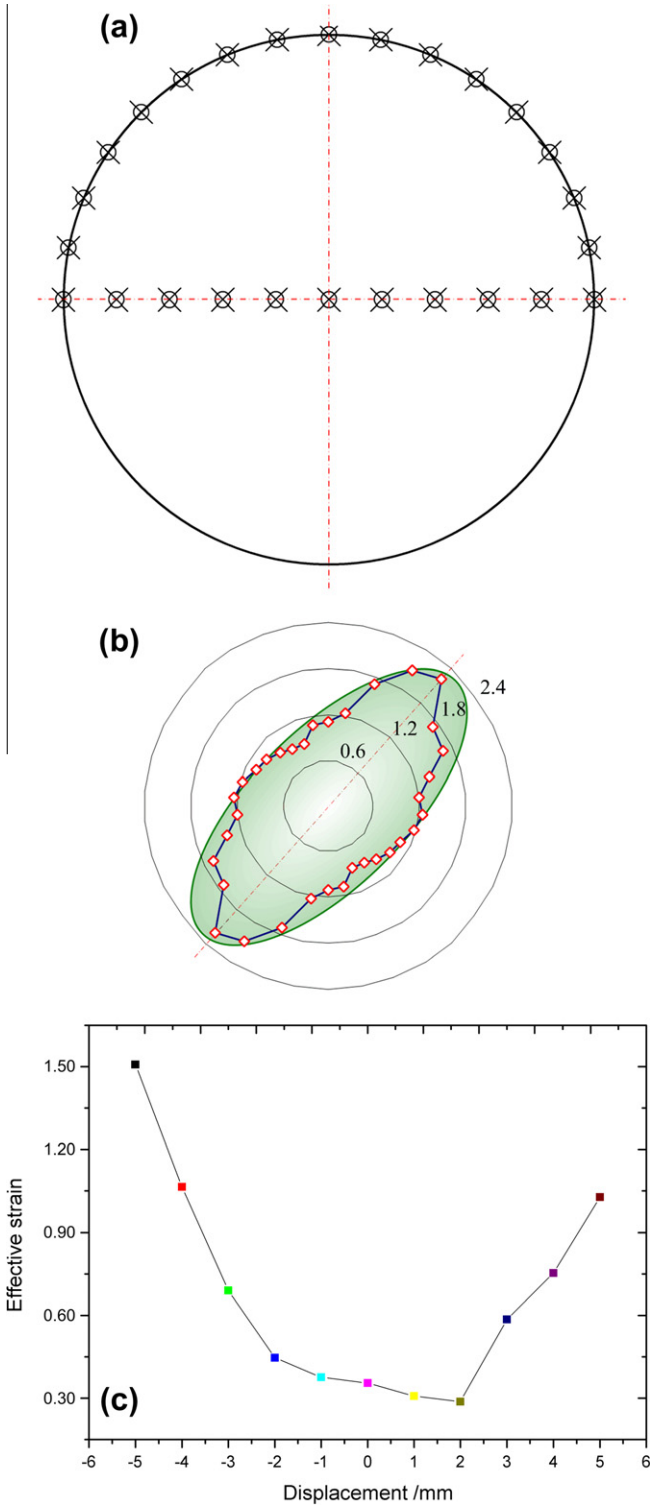

Fig. 5. Effective strain of tracking points: (a) positions of tracking points; (b) circumferential direction and (c) radial direction.

die channel. The different degrees of deformation maybe lead to significant differences in microstructures and mechanical properties for processed materials [2].

4.3. Flow net

ECSEE, like HPT and TE, unlike ECAP, is mainly characterized by the intense material flow being deformed within the workpiece cross-section. To confirm the material transverse flow, the deformation of flow grid is analyzed (Fig. 6). The transverse box at different positions presents different forms. The grid in circumferential direction, such as the representative grids I and III, has a most obvious change, and the square transforms into the unequal-sides parallelogram or the diamond. This observation of deformed flow net is related to the simple shear deformation mechanism [26]. Segal [27] proposed that the simple shear played a very important role in the SPD process. Notably, the central square grid just rotates a certain angle (a representative grid II), similar to that during elongation, according to Beygelzimer's two-stage character of a simple shear deformation hypothesis [28]. Compared to the only rotation of central grids, the ones in the circumferential direction, not only rotate, but also change the sides (a representative grid III). This is other evidence that the ECSEE-ed workpiece undergoes very high strain at the circumferential area and less at the center. The difference between two regions is due to the inhomogeneous ECSEE deformation. These different regions suffered different shear strain come from the unique elliptical cross-section of ECSEE die channel. The different regions of major-axis and minor-axis could be subjected to different degrees of shear strain. Obviously, the central area is imposed to a relative scarce shear strain. Such flow net change indicates that large amount of redundant shear strain is mainly applied in the circumferential area of the workpiece. The increase of inhomogeneous deformation may be eliminated by increasing the ECSEE pass.

4.4. Microstructure examination

Fig. 7 shows the metallographs on the cross-section of processed workpieces. The grain sizes of the segment 1 (the as-deformed workpiece) are in the range of 10–50 μm (Fig. 7a). Annealed twins are partially observed in the coarse grains. Compared to the as -deformed workpiece, the grains of the circumferential area are stretched, and even broken, appearing a different degree of deformation belt due to the severe shear plastic deformation (the right of Fig. 7b). The grains of shear band sections were obviously refined, which also appeared in the observation of TE-ed sample's microstructure [29].

In contrast, the inside ones have a little refinement due to the scarce shear strain suffered (the left of Fig. 7b). According to the simulated effective strain distribution, the observations indicate that the inhomogeneous deformation pattern of a decrease trend is from the circumferential area to the central area on the cross-section. Hence, a deductive relationship between the grain refinement and the strain distribution is obvious. Furthermore, there are varying degrees of refinements in different circumferential parts, e.g. the obvious shear bands and grain refinements are observed in the position A, while the phenomenon is unobvious in the position B (Fig. 7c). The reason seems to relate to the quantity of shear deformation suffered in different positions. Maybe the position A locates the major-axis area of the elliptical cross-section, whereas the position B does not possibly locate. The inhomogeneous refinement is ascribed to the inhomogeneous deformation (Fig. 4). Compared to the observations of the positions of A and B, a slight change of grain size (only refined to 5–30 μm) occurs in the position C, namely the central area of the segment 3 (Fig. 7d). But for the circumferential direction, the grains are significantly refined to 1–10 μm in the position D (Fig. 7e). The obvious difference between circumferential area and central area is observed in the segment 3. Accordingly, it infers that increasing the deformation passes may improve the regiment effect (only one pass of process in this paper).

After one pass of ECSEE, the macrostructure was significantly refined but was inhomogeneous, relating to the strain gradient imposed by the ECSEE torsion die channel geometry. The inhomoge-

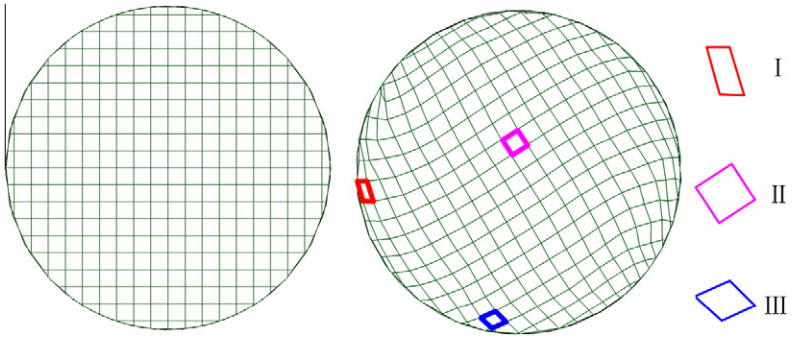

Fig. 6. Flow net of the transverse pattern.

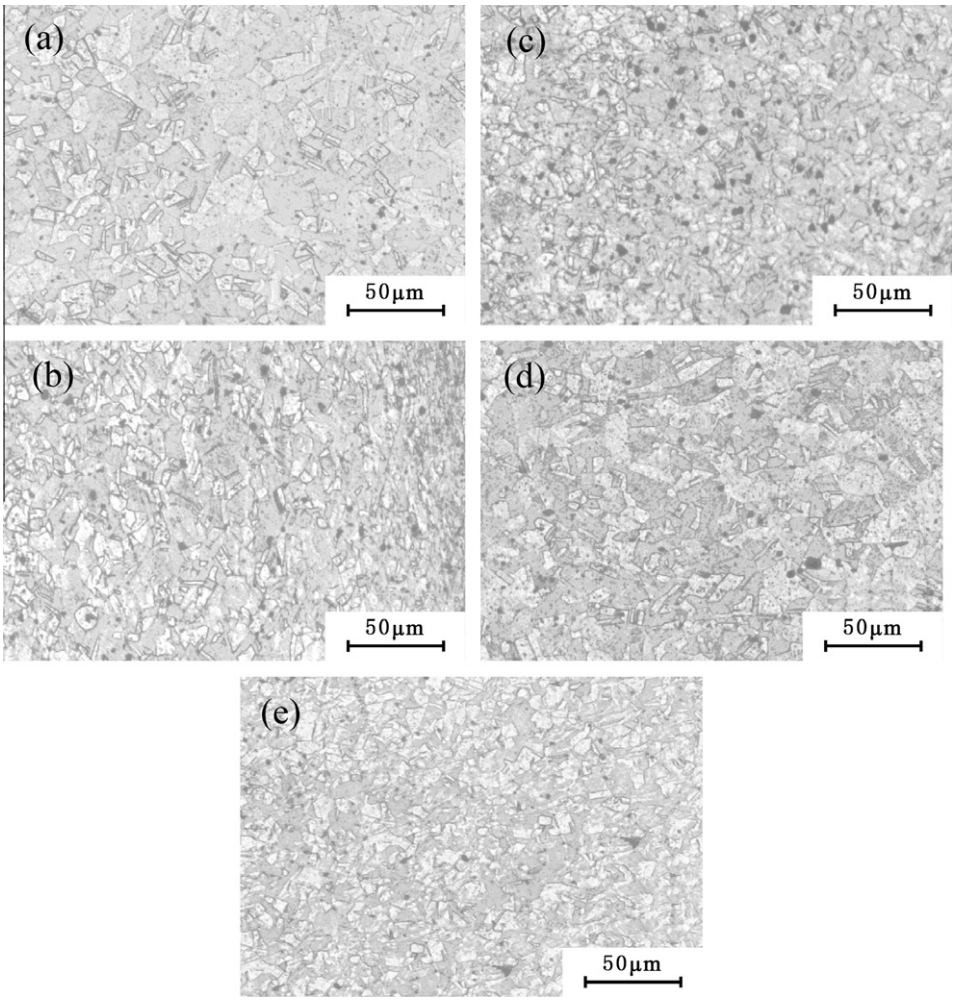

Fig. 7. Metallographic observations of the workpieces' cross-sections: (a) segment 1, (b) position A, (c) position B, (d) position C and (e) position D.

neous structural distribution of ECSEE-ed materials is a more important question to be addressed. Similarly, a grain refinement gradient was found in TE-ed metals with enhancing the high ductility [30]. Besides, the evolution of structure observed is in a reasonable agreement with the results reported of HPT method [31].

4.5. Hardness variation

In view of the correlation between the hardness measurements and the internal deformation, thereby hardness measurements were performed to provide a simple and expedient procedure for reaching conclusions on the deformation characteristics and the degree of internal homogeneity within the processed workpieces. Fig. 8a shows the hardness distribution along the circumferential direction on the cross-section of the segment 2. The red[1] curve represents the real value measured, and the blue curve is a virtual symmetric one for the investigation. The measured value for the as-deformed workpiece is ~40 Hv. As shown in Fig. 8a, the elliptical shape of hardness distribution is similar to that of the elliptical

[1] For interpretation of color in Figs. 1, 3–6, 8 the reader is referred to the web version of this article.

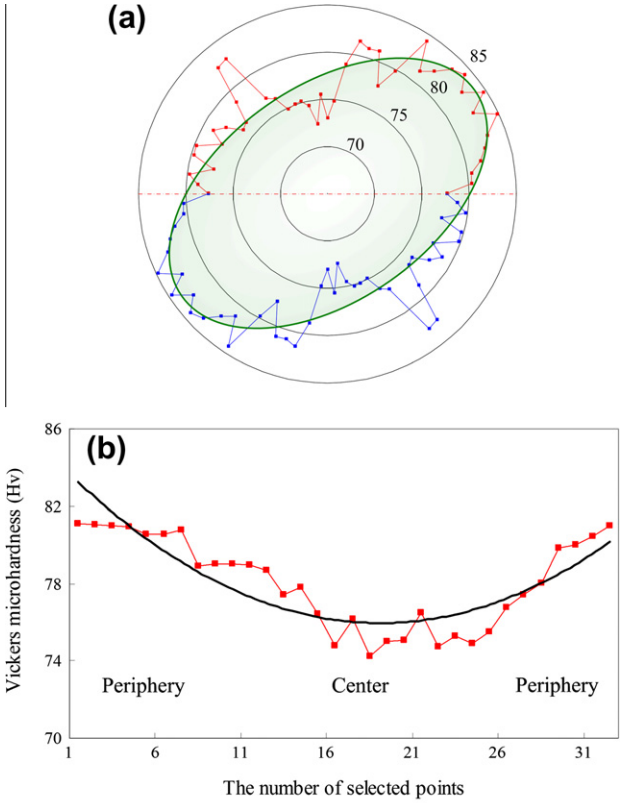

Fig. 8. Hardness of the segment 2 cross-sections: (a) circumferential direction and (b) radial direction.

cross-section of ECSEE die channel. The maximum value of ~85 Hv is achieved at the both ends of the major-axis of elliptical cross-section; while the minimum one of ~72.5 Hv is achieved at both ends of the minor-axis. Compared to the as-annealed workpiece, the hardness is greatly improved for processed workpieces. The distribution characteristic of ellipse shape is also consistent with that of effective strain distribution in the previous simulation (Fig. 5b). Explanation of the similarity between the distribution of hardness and effective strain is ascribed the similar influence from the total torsional strain [25].

Fig. 8b shows the radial hardness distribution along a straight line through the center point of the cross-section of segment 2. The value close to the periphery area, corresponding to the circumferential area of the cross-section, is significantly higher than that of the central area. The previous document [25] reported that the microhardness values were generally non-uniform across the diameters of HPT-ed samples and there were lower hardness values in the center of the disk. There is a similar hardness distribution characteristic between ECSEE and HPT. Both ends of hardness value are not symmetrically distributed due to the unsymmetrical cutting and the inhomogeneous deformation of ECSEE. The trend of hardness distribution decreasing from the circumferential area to the central area is also similar to the simulated effective strain distribution (Fig. 5c).

5. Conclusions

(1) A 3D finite element model was established to analyze the deformation characteristic of ECSEE for pure copper workpieces. Simulated results indicated that the effective strain distribution of ellipse shape shows a decreasing trend from the circumferential area to the central area on the cross-section of processed workpieces. This non-uniform shear deformation plays an essential role in the grain refinement of ECSEE processing.

(2) To verify the simulation results, a single-pass of ECSEE was executed for the pure copper material, and the metallographic and hardness homogeneity were measured. Metallographic observation indicates that the grains are refined from 10–50 μm to 1–10 μm in the circumferential area. In addition, the hardness value of the circumferential area is higher than that of the central area on the cross-section. The distribution characteristic of refinement and hardness are both consistent with that of the simulated effective strain.

(3) The numerical and experimental results provided useful theoretical and experimental guidelines for the ECSEE technique, which as a novel SPD method appears very promising for obtaining UFG materials, thus extensive basic researches on ECSEE are significant to fabricate UFG and even nanostructural materials.

Acknowledgements

The authors are very grateful for the support received from the Aeronautical Science Foundation of China under Grant No. 2011ZE53059.

References

[1] Valiev RZ. Nanostructuring of metals by severe plastic deformation for advanced properties. Nat Mater 2004;3:511–6.
[2] Valiev RZ, Islamgaliev RK, Alexandrov IV. Bulk nanostructured materials from severe plastic deformation. Prog Mater Sci 2000;45:103–9.
[3] Tolaminejada B, Dehghanib K. Microstructural characterization and mechanical properties of nanostructured AA1070 aluminum after equal channel angular extrusion. Mater Des 2012;34:285–92.
[4] Horita Z, Langdon TG. Achieving exceptional superplasticity in a bulk aluminum alloy processed by high-pressure torsion. Scripta Mater 2008;58:1029–32.
[5] Richert M, Liu Q, Hansen N. Microstructural evolution over a large strain range in aluminium deformed by cyclic-extrusion-compression. Mater Sci Eng A 1999;260:275–83.
[6] Beygelzimer Y, Varyukhin V, Synkov S, Orlov D. Useful properties of twist extrusion. Mater Sci Eng A 2009;503:14–7.
[7] Akbari Mousavi SAA, Shahab AR, Mastoori M. Computational study of Ti-6Al-4V flow behaviors during the twist extrusion process. Mater Des 2008;29:1316–29.
[8] Hosseini SA, Manesh HD. High-strength, high-conductivity ultra-fine grains commercial pure copper produced by ARB process. Mater Des 2009;30:2911–8.
[9] Khodabakhshi F, Kazeminezhad M. The effect of constrained groove pressing on grain size, dislocation density and electrical resistivity of low carbon steel. Mater Des 2011;32:3280–6.
[10] Ferrasse S, Segal VM, Alford F, Kardokus J, Strothers S. Scale up and application of equal-channel angular extrusion for the electronics and aerospace industries. Mater Sci Eng A 2008;493:130–40.
[11] Lowe TC, Zhu YT. Commercialization of nanostructured metals produced by severe plastic deformation processing. Adv Eng Mater 2003;5:373–8.
[12] Mani B, Jahedi M, Paydar MH. A modification on ECAP process by incorporating torsional deformation. Mater Sci Eng A 2011;528:4159–65.
[13] Parimi AK, Robi PS, Dwivedy SK. Severe plastic deformation of copper and Al–Cu alloy using multiple channel-die compression. Mater Des 2011;32:1948–56.
[14] Zangiabadi A, Kazeminezhad M. Development of a novel severe plastic deformation method for tubular materials: Tube Channel Pressing (TCP). Mater Sci Eng A 2011;528:5066–72.
[15] Bouaziz O, Estrin Y, Kim HS. A new technique for severe plastic deformation: the cone-cone method. Adv Eng Mater 2009;11:982–5.
[16] Khoddam S, Farhoumand A, Hodgson PD. Upper-bound analysis of axi-symmetric forward spiral extrusion. Mech Mater 2011;43:684–92.
[17] Lu LW, Liu TM, Chen Y, Wang LG, Wang ZC. Double change channel angular pressing of magnesium alloys. Mater Des 2012;35:138–43.
[18] Alihosseini H, Zaeem MA, Dehghani K. A cyclic forward–backward extrusion process as a novel severe plastic deformation for production of ultrafine grains materials. Mater Lett 2012;68:204–8.
[19] Varyukhin V, Beygelzimer Y, Synkov S, Orlov D. Application of twist extrusion. Mater Sci Forum 2006;503–504:335–9.

[20] Djavanroodi F, Ebrahimi M. Effect of die parameters and material properties in ECAP with parallel channels. Mater Sci Eng A 2010;527:7593–9.
[21] GB/T 228–2002. Metallic materials-tensile testing at ambient temperature. China Standard Press; 2002.
[22] Islamgalievd RK, Buchgraber W, Kolobov YR, Amirkhanov NM, Sergueeva AV, Ivanov KV, et al. Deformation behavior of Cu-based nanocomposite processed by severe plastic deformation. Mater Sci Eng A 2001;319–321:872–6.
[23] Zhao Y, Guo HZ, Shi ZF, Yao ZK, Zhang YQ. Microstructure evolution of TA15 titanium alloy subjected to equal channel angular pressing and subsequent annealing at various temperatures. J Mater Process Technol 2011;211:1364–71.
[24] GB/T 4340.1-2009. Metallic materials-Vickers hardness test-Part I: Test method. China Standard Press; 2009.
[25] Zhilyaev AP, Nurislamova GV, Kim BK, Baró MD, Szpunar JA, Langdon TG. Experimental parameters influencing grain refinement and microstructural evolution during high-pressure torsion. Acta Mater 2003;51:753–65.
[26] Segal VM. Materials processing by simple shear. Mater Sci Eng A 1995;197:157–64.
[27] Segal VM. Severe plastic deformation: simple shear versus pure shear. Mater Sci Eng A 2002;338:331–44.
[28] Beygelzimer Y, Valiev RZ, Varyukhin V. Simple shear: double-stage deformation. Mater Sci Forum 2011;667–669:97–102.
[29] Beygelzimer Y, Orlov D, Korshunov A, Synkov S, Varyukhin V, Vedernikova I, et al. Features of twist extrusion: method, structures & material properties. Solid State Phenom 2006;114:69–78.
[30] Orlov D, Beygelzimer Y, Synkov S, Varyukhin V, Tsuji N, Horita Z. Plastic flow, structure and mechanical properties in pure Al deformed by twist extrusion. Mater Sci Eng A 2009;519:105–11.
[31] Horita Z, Langdon TG. Microstructures and microhardness of an aluminum alloy and pure copper after processing by high-pressure torsion. Mater Sci and Eng A 2005;410–411:422–5.